Time Variation of Ocean Temperatures and Its Relation to Internal Waves and Oceanic Heat Flow Measurements[1]

W. H. K. LEE

Institute of Geophysics and Planetary Physics, University of California, Los Angeles

C. S. COX

Scripps Institution of Oceanography, University of California, San Diego

Recent data from four oceanic stations in the northeastern Pacific permit time series analysis of ocean water temperature at depths extending from the surface to the bottom. At three of the stations, data taken at about monthly intervals for 12 years from the surface down to depths of 1000 meters are available. At the fourth station, data were taken at 5-minute intervals for 14 days at 15 depths, the lowest being just above the sea floor. The computation of the temperature spectra is especially adapted to the analysis of time series with missing data. Short-period variations of ocean water temperatures (from depths 85 to 3803 meters) are dominated by a semidiurnal periodicity. The results suggest that vertical motions of the ocean water associated with this 'internal tide' are of the order of 10 meters in amplitude. Semidiurnal temperature flucutations of ocean waters may also introduce some errors in the measurement of heat flow through the ocean floor, especially in rough topography. Long-period temperature variations at shallow depths are dominated by the annual periodicity, which becomes less pronounced below a few hundred meters. The results suggest that reliable heat flow measurements through the ocean floor may be made in water as shallow as 200 meters, provided that observations are made below about 3 meters in the sediment.

INTRODUCTION

The study of ocean water temperatures is fundamental in oceanography. For example, circulation patterns in the oceans are inferred from the geographical distribution of water temperatures with depth; and techniques of measuring heat flow through the ocean floor are based on the observed constancy of water temperatures in the deep ocean. However, because of the lack of data, little is known about the time variation of deep ocean water temperatures. In this paper we present the time series analysis of four sets of ocean water temperature records and discuss the results in relation to internal wave and oceanic heat flow measurements.

PREVIOUS WORK

Rossby [1937–1938] has demonstrated theoretically that there should be a great deal of thermal unrest in the deep ocean because internal inertial gravity wave motions are induced in the deep stratified layers of the sea in response to transient wind stresses. *Rattray* [1964] and *Longuet-Higgins* [1965] have extended the theoretical treatment to planetary waves and called attention to the possibility that the deep irregular currents observed by *Swallow* [1961] and *Crease* [1962] are the expression of these waves. *Defant* [1932, 1950] has suggested that the internal tidal waves are widespread in the oceans and has presented many analyses of short series observations as evidence. *Haurwitz et al.* [1959] analyzed temperature observations from depths of 50 and 500 m off Castle Harbor, Bermuda Islands. Their data, extending from December 1954 to October 1955, are the longest almost continuous time series of temperature records, and may be representative of typical oceanic thermal conditions because they were recorded from the flanks of an oceanic island. At low frequencies, their temperature spectra possibly show small peaks near the semidiurnal tidal frequency (amplitude about 0.1°C) and (at 500 m depth) near the inertial or diurnal tidal frequency.

[1] Publication 465, Institute of Geophysics and Planetary Physics, University of California, Los Angeles, and Contribution of Scripps Institution of Oceanography, New Series.

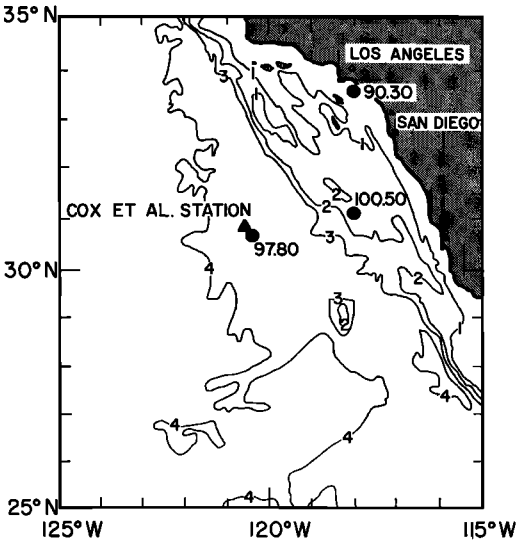

Fig. 1. Station locations for time series analysis of water temperature.

Aside from these peaks and a very broad maximum of the 500-m spectra centered at 0.5 cph, the spectra decrease monotonically with increasing frequency.

Present Data

The station locations of the four sets of ocean water temperature records studied are shown in Figure 1. For short-period variations the temperature data are from *Cox et al.* [1965], who measured the temperature (to a short-term precision of ±0.002°C) at 15 depths from 85 to 3803 m every 5 minutes, for 14 days (December 5 to 19, 1964), at a location 370 km southwest of San Diego in water 3836 m deep. After ignoring a few per cent of the original data which are missing or obviously in error, we have analyzed the hourly averages (normalized to zero mean value) with almost complete coverage in the time domain studied. Statistics of the 15 series studied are summarized in Table 1.

An extensive search of existing data (e.g., *Oceanic Observations in the Pacific,* 1949–1960) revealed that only a few hydrographic stations near the station of *Cox et al.* [1965] have a sufficient number of temperature data over the last 15 years for time series analysis. Station 97.80 (30°35′N, 120°30′W) is almost identical in location with that of *Cox et al.* [1965] (30°44′N, 120°41′W), and the data include readings for six depths between 0 and 500 m (Table 2). Station 90.30 is similar, except that it is located just off Los Angeles. The data from station 100.50 consist of readings from as deep as of 1000 m. The temperatures (measured to ±0.02°C) at all these stations have been sampled at approximately monthly intervals between 1950 and 1960. However, 20 to 60% of the data are missing and the data were not taken at equal time intervals. The original data were plotted and values were interpolated between data points. The analyzed values were then taken at 30-day intervals, gaps being left where the original data were insufficient, and each series was also normalized to zero mean value. Statistics of the 18 series studied are summarized in Table 2.

Analysis of Time Series with Missing Data

The main difficulty in time series analysis is the treatment of missing data. The usual practice is to interpolate through the data gaps in order to have an unbroken record, as required by the analysis. Where many data are missing (e.g., hydrographic station data in this paper), such a procedure can introduce spurious results (due to the scheme of interpolation) which contaminate the actual spectrum. We have attempted to minimize this danger by the following computation procedure which has two advantages: (1) it gives correct results if few or no data are missing and (2) it signals those sections of the spectrum where the data are insufficient by giving negative spectral estimates, which are obviously impossible.

The usual method of time series analysis is that described by *Blackman and Tukey* [1958]. For a time series $X(t_1)$, $X(t_2)$, . . . , $X(t_n)$, where $\Delta t = t_i - t_{i-1}$, the autocovariance function at lag τ is computed by

$$C(l) = \left(\frac{1}{n-l}\right) \sum_{i=l+1}^{n} X(t_{i-l})X(t_i) - \left(\frac{1}{n-l}\right)^2 \sum_{i=l+1}^{n} X(t_{i-l}) \sum_{i=l+1}^{n} X(t_i) \qquad (1)$$

for $l = 0, 1, 2, \ldots, m$; and $\tau = l\Delta t$.

In our method, where there are data gaps in the time series, the sum of lagged products includes only those products that are available, and the divisor $(n-l)$ is modified to be num-

TABLE 1. Statistics of Data of Cox et al. [1965]*

Series	Depth, m	N†	Mean Temperature, °C	RMS Value for the Entire Spectrum, °C	RMS Value for the Semidiurnal Peak, °C	Mean Temperature Gradient, °C/km	RMS Vertical Motion at Semidiurnal Frequency, m
1	85	320	12.0	0.507	0.233	57	4.1
2	128	314	9.8	0.354	0.164	30	5.5
3	175	316	8.7	0.096	0.059	21.5	2.7
4	230	313	7.7	0.104	0.072	14.0	5.1
5	320	315	6.8	0.095	0.078	7.9	9.9
6	432	313	6.15	0.082	0.048	6.9	7.0
7	565	319	5.25	0.069	0.031	5.0	6.2
8	720	320	4.65	0.034	0.016	4.3	3.7
9	890	312	4.10	0.036	0.026	3.0	8.7
10	1080	311	3.70	0.036	0.026	2.7	9.6
11	1330	317	3.10	0.048	0.024	2.4	10.0
12	1610	311	2.60	0.019	0.014	1.70	8.2
13	1990	307	2.05	0.015	0.009	1.09	8.3
14	2500	306	1.80	0.014	0.006	0.44	1.4
15	3803	308	1.55	0.012	0.003	0.22	1.4

* Station located at 30°44.0′ N, 120°40.8′ W; 3836 meters water depth.
† N is the number of hourly averages available for the analysis. If no data are missing, $N = 325$.

TABLE 2. Statistics of Hydrographic Station Data

Station	Series	Depth, m	N*	Mean Temperature, °C	RMS Value for the Entire Spectrum, °C	RMS Value for the Annual Peak,† °C
	1	0	55	16.97	1.65	1.27
97.80	2	100	55	12.80	1.53	
(30°35′N,	3	200	54	8.72	0.29	
120°30′W,	4	300	54	7.30	0.20	
3843 m	5	400	51	6.41	0.18	
water	6	500	51	5.82	0.15	
depth)						
90.30	1	0	58	16.43	2.13	2.10
(33°25′N,	2	100	58	10.05	0.98	0.58
117°55′W,	3	200	57	8.87	0.51	0.18
600 m	4	300	57	8.03	0.36	0.11
water	5	400	57	7.17	0.23	0.11
depth)	6	500	45	6.45	0.17	0.05
100.50	1	0	76	16.55	1.78	1.38
(31°00′N,	2	200	75	8.56	0.39	0.12
118°08′W,	3	400	74	6.75	0.29	
1740 m	4	600	54	5.51	0.18	
water	5	800	35	4.64	0.09	
depth)	6	1000	33	3.99	0.08	

*N is the number of monthly averages available for the analysis. If no data are missing, $N = 125$ for station 97.80, $N = 112$ for station 90.30, and $N = 119$ for station 100.50.
† Where annual peak in the spectra is not pronounced, the rms value has not been estimated.

ber of lagged products entering into the sum at that lag.

The spectral density at frequency f is given by

$$P(f) = 2\Delta t\left[A(0) + 2 \sum_{l=1}^{m-1} A(l) \cdot \cos(2\pi f l \Delta t) + A(m) \cos(2\pi m f \Delta t)\right] \quad (2)$$

for $f = 1/(2m\Delta t, \ldots, 1/(2\Delta t,$ where

$$A(l) = W(l)C(l) \quad (3)$$

For the data of *Cox et al.* [1965], $W(l)$ is taken as the 'Tukey' lag window [*Blackman and Tukey,* 1958, p. 14] because the data gaps are few. For the hydrographic station data which have frequent data gaps, the 'Parzen' lag window [*Jenkins,* 1961, p. 146] is used because it does not have negative side bands. Consequently, negative spectral estimates can be introduced only by the data gaps. These negative values indicate whether time series can be suitably analyzed for a series with so many data gaps, as mentioned above.

For the time series by *Cox et al.* [1965] the original data were first reduced to hourly values by taking 1-hour means. The modified series $X'_n(t)$ have a Nyquist frequency $f_N = 0.5$ cph. They were then 'prewhitened' by applying the difference filter

$$X_n(t) = X_n'(t + 1 \text{ hour}) - X_n'(t) \quad (4)$$

in order to produce time series with nearly uniform spectra. This procedure was found to be necessary to prevent contamination of the spectral intensities at medium frequency by side bands of the zero frequency peak. Finally, the spectra were computed and corrected by dividing by the filter factor

$$4 \sin^2 [\pi f/(2f_N)] \quad (5)$$

to recover the correct shape of the spectra of the original data. The lag interval was taken to be 1 hour, and 50 spectral estimates were evaluated.

For the hydrographic station data, such prewhitening was found to be unnecessary because the zero frequency peak was small. The lag interval was taken to be 30 days, and 30 spectral estimates were evaluated.

Results

The temperature spectra are shown on logarithmic scales in Figures 2 and 3. The high-frequency data show weak diurnal peaks (0.04 cph) and strong semidiurnal peaks (0.08 cph) superimposed on continuous backgrounds that rise steeply toward zero frequency. The semidiurnal peaks usually rise several times higher than the backgrounds even at the greatest depths. The rms temperature fluctuations contributed by those peaks are summarized in Table 1. The continuous backgrounds of the four lowest spectra (series 12–15) have about the same intensity at frequencies below 0.03 cph. This may represent the spectrum of instrumental noise and drift. It is clear that the semidiurnal peaks in the temperature spectra from these deepest records are well above instrumental noise level, as are all parts of the spectra for shallower depth. The strength of the semidiurnal peaks relative to the diurnal peaks is consistent with the behavior of internal waves poleward of the inertial latitude (30°)

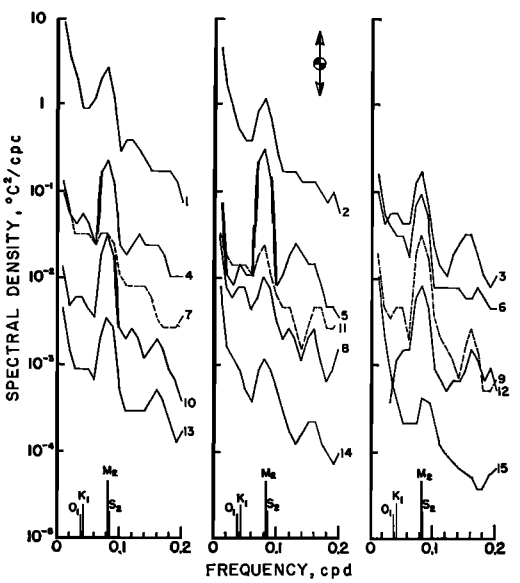

Fig. 2. Spectra of the temperature data of *Cox et al.* [1965]. Series number is indicated at the right and corresponds to depths given in Table 1. The double-headed arrow shows the total range of 95% confidence limits derived from 13 degrees of freedom [*Munk et al.,* 1959, p. 291]. Lines on the abscissa show the frequency of tidal constituents. Lengths are proportional to equilibrium amplitudes.

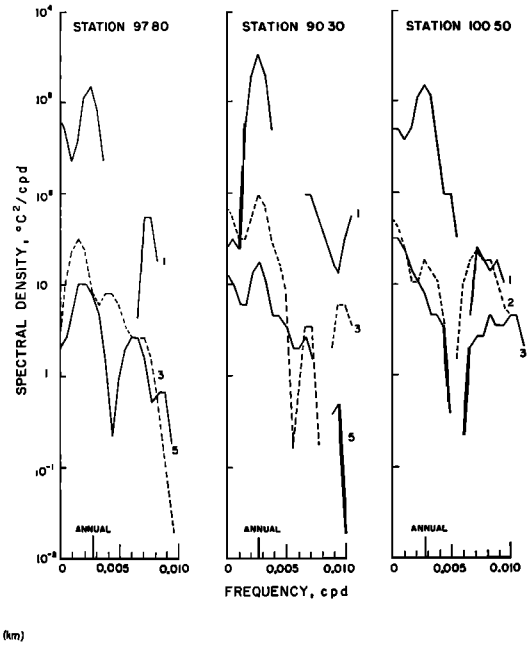

Fig. 3. Spectra of hydrographic station temperature data. Series number is indicated at the right and corresponds to depths given in Table 2. Gaps in the curve are due to negative spectral estimates introduced by missing data (see text).

for diurnal waves. This follows because the phase velocity of internal waves is proportional to $(f^2 - 4 \sin^2 \theta/1 \text{ day}^2)^{-1/2}$, where f is the frequency of waves and θ the latitude. We conclude that at these frequencies the observations show internal waves related to tidal flow. The nature of the continuous backgrounds is uncertain.

The low-frequency spectra (Figure 3) show, at the surface and for all three stations, an expected large peak at the annual frequency. The annual peak is fairly well preserved to 400 or 500 m depth at station 90.30 (near the coast). It disappears at about 400 m at station 100.50 (farther away from land) and is not recognizable at station 97.80 (in the open ocean). Since the incoming solar radiation is rapidly absorbed in the first few meters of ocean water, the annual temperature oscillation at greater depths must indicate mixing and/or changes of circulation. The data show that these changes extend to only a few hundred meters. Near shore (e.g., station 90.30), where winds are weak, the mixed layer at the surface is thin and consequently undergoes larger temperature fluctuations than off shore (e.g., stations 100.50 and 97.80), where winds are stronger and the mixed layer is thicker. Consequently, at the sea surface the annual spectral peak at station 90.30 is much larger than that at the other two off-shore stations (see Figure 3). The rms temperature fluctuations contributed by the annual peak are summarized in Table 2.

Since the low-frequency spectra are derived from data at monthly intervals, they are subjected to aliasing due to high-frequency fluctuations. We can estimate the highest-frequency part of the aliasing by analyzing the data of *Cox et al.* [1965]. The effect of such aliasing is to introduce an almost 'white' noise into the spectra. For example, a spectral estimate of this noise level for series 3 of station 97.80 is about 0.6° C²/cpd, which is well below curve 3 of Figure 3. There may be additional contributions to the aliasing by fluctuations of periods between 4 and 60 days that cannot be discovered from the present data, but it seems unlikely that such aliasing will be severe enough to contaminate the annual peaks in Figure 3.

Relation to Internal Waves

Oscillations of temperature T recorded at a fixed depth can be interpreted in terms of water motions according to

$$\kappa\nabla^2 T - \delta T/\delta t = u(\partial T/\partial x) + v(\partial T/\partial y) + w(\partial T/\partial z) \qquad (6)$$

Here, κ, δT, u, v, and w are the thermal diffusivity, temperature oscillations, and the components of water velocity at the point of observation. Since κ is negligibly small, $\kappa\nabla^2 T$ can be neglected in (6). It is usually assumed that the horizontal temperature gradient ($\partial T/\partial x$, $\partial T/\partial y$) is small and that $\partial T/\partial z$ can be replaced by its value $\langle \partial T/\partial z \rangle$ averaged over a rather great depth range. This yields

$$w \approx -(\delta T/\delta t)/\langle \partial T/\partial z \rangle \qquad (7)$$

The vertical motions associated with the temperature oscillations are inferred from equation 7 (cf. Figure 4). The difference between the real temperature gradient and $\langle \partial T/\partial z \rangle$ may be the principal source of error in this investigation.

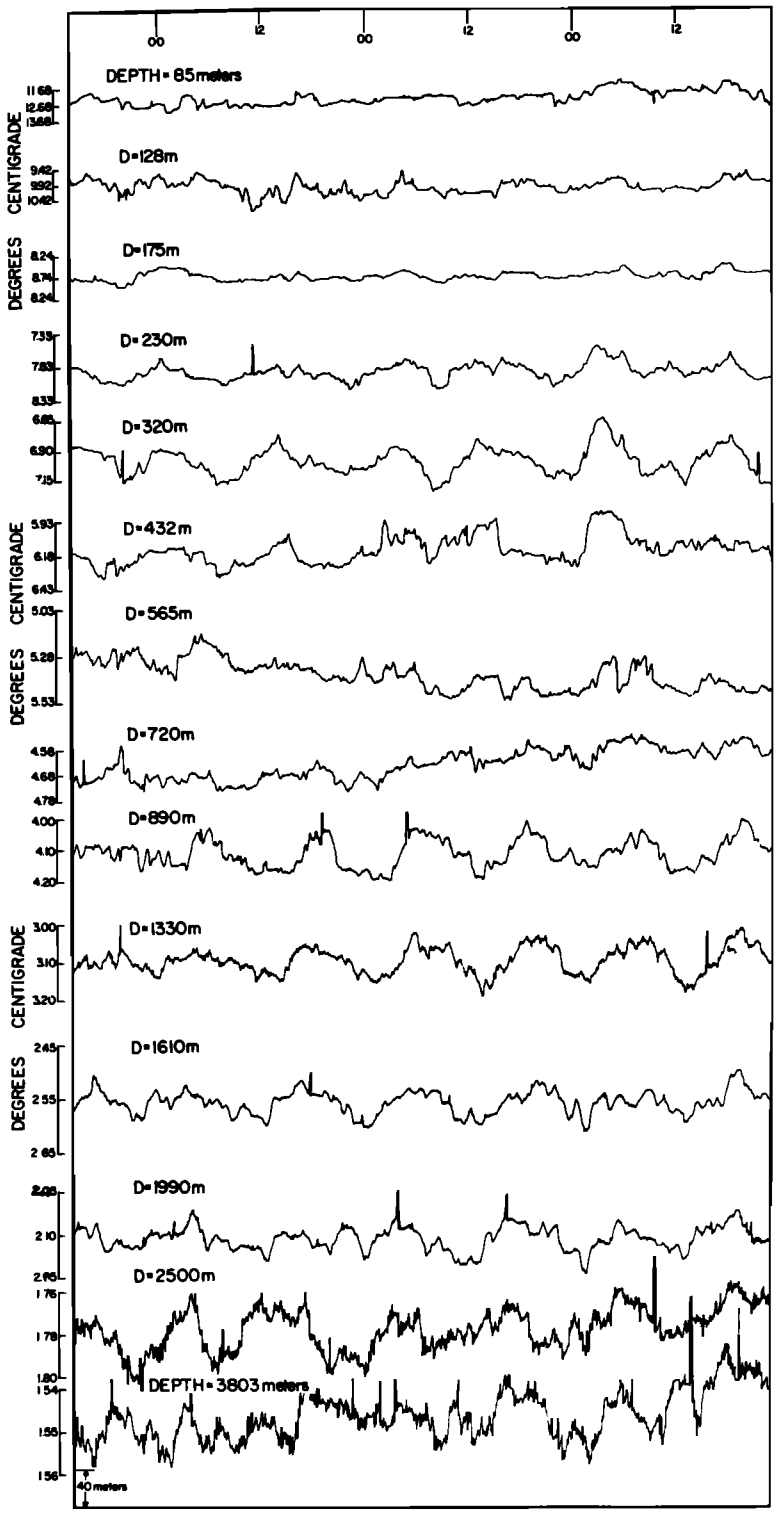
00
12
00
12
00
12
DEPTH = 85 meters
D=128m
D=175m
D=230m
D=320m
D=432m
D=565m
D=720m
D=890m
D=1330m
D=1610m
D=1990m
D=2500m
DEPTH = 3803 meters
CENTIGRADE
DEGREES
40 meters

There is increasing evidence from our own experience that a microscale of temperature layering extends to great depths, causing the temperature to decrease downward in a series of irregular steps. The vertical motions of water, then, are translated in an extremely nonlinear manner into water temperature fluctuations at a fixed depth. One expects that the semidiurnal water motions will produce 'fundamental' water temperature fluctuations at 0.08 cph and 'overtones' at about 0.16 cph, 0.25 cph, ... Evidence of the first overtones is shown in the spectra of series 3, 8, 9, 10, 12, 13, and 14 in Figure 2.

We can suppress this source of error in the interpretation by using only the fundamental to estimate vertical motion amplitudes in (7). The mean temperature gradients and rms semidiurnal vertical motions are listed in Table 1. The largest oscillations occur at mid-depth. It has been verified that these apparent vertical motions are many times larger than any possible motions of the thermometers themselves [*Cox et al.*, 1965].

The semidiurnal motions are much larger than can be caused by the tidal rise and fall of the sea surface. They are consistent with the behavior of internal waves, which should have maximum motions within the ocean and die away toward the surface and bottom. The temperature fluctuations at the bottom may be the expression of orbital currents flowing over the inclined sea floor.

The fact that the vertical motions are many times larger than equilibrium tidal heights (about 0.4 m for M_2 at 30°N) suggests that these internal waves are not generated directly by gravitational attraction as proposed by *Defant* [1950]. Although, in theory, waves of far higher amplitude than the equilibrium value could be generated in an inviscid medium by a resonance mechanism, this would imply an inadmissibly low damping. Internal tides can also be generated by interaction of the surface tide with the rough sea floor [*Cox and Sandstrom*, 1962]. The present observations are not sufficient to establish the mechanism of generation, but they at least raise the possibility that important temperature fluctuations of tidal period are widely present on the sea floor and may be more common in regions of rough sea floor topography. We would expect the amplitude of temperature oscillations to increase on sea floor ridges and shoals for two reasons: (1) The temperature gradient decreases with depth; therefore a given vertical water motion produces more temperature variation. (2) The flux of energy into internal tides by the mechanism of Cox and Sandstrom will be large in such places. The observations by *Reid* [1956] of large temperature oscillations over the continental slope off the California coast is indicative of these effects.

Relation to Oceanic Heat Flow Measurements

Techniques of measuring heat flow through the ocean floor are based on the assumption that the bottom water temperature in the deep oceans is constant with time. If this assumption is valid, the ocean floor should reach a steady thermal state. Therefore, values of steady heat flow can be obtained by measuring the temperature gradient and thermal conductivity in the upper few meters of the sediment. Initial justification of this assumption has been based on several cases of repeated temperature observations in the deep oceans (>4 km depth) which gave values within the instrumental error limits (±0.02°C). Using a 5-m probe with three thermojunctions, *Bullard and Day* [1961] showed rather minor differences in temperature gradient between the top and bottom halves of the probe. The evidence

Fig. 4. Water temperature records from *Cox et al.* [1965]. The figure shows about one-fourth of the available time series. The scales at the left of each trace show the temperature fluctuation. They have been adjusted so that one ordinate unit is proportional to the inverse of the mean temperature gradient at corresponding depths. Therefore the temperature oscillations can be readily visualized in terms of vertical oscillation with a uniform scale of 40 m per division as shown by the double-headed arrow to the left and below the 3803-m trace. A deflection of a trace upward (temperature dropping) corresponds nominally to a movement of water upward around the transducer. Occasional sharp spikes on all traces are the result of incorrect transcription of some digits in the recording, and they have been eliminated before time series analysis.

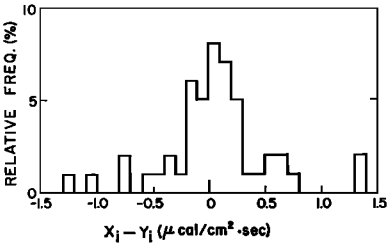

Fig. 5. Histogram of $\{x_i - y_i\}$ for pairs of heat flow stations less than 10 km apart at sea with heat flow values x_i and y_i [from *Lee and Uyeda,* 1965, Figure 2].

of the multiprobe techniques [*Von Herzen and Langseth,* 1965] also demonstrated that the heat flow is generally constant with depth and implied that the bottom water temperature variations are not generally important. This premise is further supported by the general agreement of results of the Scripps probe technique with the preliminary Mohole site measurements to a depth of 154 m [*Von Herzen and Maxwell,* 1964].

At present more than 1500 heat flow observations have been made at sea, which have recently been reviewed by *Lee and Uyeda* [1965]. Although the pattern of heat flow averages is correlated with major geological features, we are puzzled by large heat flow variations over short distances, despite what has been said in the previous paragraph. For example, Figure 5 shows the histogram of $\{x_i - y_i\}$, $i = 1, 2, \ldots, n$, for pairs of heat flow stations that are less than 10 km apart at sea and have heat flow values of x_i and y_i. Pairs of such stations at sea are almost indistinguishable in position because of navigation uncertainties. However, the range of $\{x_i - y_i\}$ is almost ± 1.5 μcal/cm^2 sec, even though the average of individual heat flow values is about 1.5 μcal/cm^2 sec.

Many of these heat flow variations over short distances may be caused by steep topography, rapid variations in the sediment thickness, shallow volcanic intrusions, etc., but some may also be due to other unexpected complications. For example, *Lubimova et al.* [1965] observed superadiabatic temperature gradients in the water near the ocean bottom and have speculated about convective overturns. *Reid and Lynn* [1965] analyzed the temperature, salinity, and oxygen data obtained from 123 deep hydrographic stations off California from January 1960 to December 1963. They found that beneath the depth of temperature minimum (3 to 4 km) the water appears to be vertically homogeneous in potential temperature, salinity, and oxygen, and they concluded that such homogeneity is a consequence of heat conducted from the earth's interior causing convective overturn and mixing upward from the bottom to the depth of the temperature minimum. However, it is difficult to see how such overturn could lead to appreciable temperature fluctuations. We believe a far more important source of temperature fluctuation in depths less than 4 km is produced by the internal waves discussed in the preceding section. *Lee and Uyeda* [1965, Figures 15, 20, and 29] also demonstrated that the scatter of heat flow values is much larger in the oceanic ridges than in the basins. A partial cause may be the larger bottom water temperature variations associated with internal waves, as explained in the preceding section. In fact, we would expect the rms variations in temperature to be considerably larger in regions of oceanic ridges than at the station of *Cox et al.* [1965], where the bottom topography is very smooth. We therefore suggest that the temperature disturbances caused by internal waves may be partly responsible for the large apparent heat flow variations over short distances, especially in rough sea floors. We further suggest that the semidiurnal internal waves having vertical motions of tens of meters can aid the mixing in the oceans observed by *Reid and Lynn* [1965]. The instability in shear (see appendix) associated with such water motions near the sea floor would be expected to destroy any superadiabatic gradients that might be caused by the heat flowing from the earth's interior. Thus there may be some doubt that the superadiabatic gradients of large vertical extent reported to have been observed by *Lubimova et al.* [1965]. Furthermore, they have not been confirmed by other researchers (M. G. Langseth and A. H. Lachenbruch, private communications).

The temperature variation which is critical for oceanic heat flow measurements is that at the sea floor. If the ocean bottom is a horizontal plane or is at the depths where the adiabatic temperature zone [*Reid and Lynn,*

1965] exists, the effect of internal waves will vanish. However, the sea floor is usually sloping, so that there can be vertical velocity components induced by currents flowing at the ocean bottom which cause temperature fluctuations. At shallow depths, and especially on rough sea floor topography, the temperature fluctuations can be many times larger than that shown in Table 1 at the corresponding depth.

The effects of the short- and long-period temperature fluctuations on heat flow can be estimated from their amplitude and frequency. The temperature at depth z in the sediment due to a sinusoidal oscillation, $T_0 \cos(\omega t)$ at the sediment surface $z = 0$, is [*Carslaw and Jaeger*, 1959, section 2.8(8)].

$$T_z = T_0 \exp(-kz) \cos(\omega t - kz) \qquad (8)$$

Here, $\omega = 2\pi/P$, where P is the period; and $k = (\omega/2\kappa)^{1/2}$, where κ is the thermal diffusivity. The wavelength λ is

$$\lambda = 2\pi/k = (4\pi\kappa P)^{1/2} \qquad (9)$$

Taking $\kappa = 0.002$ cm²/sec for ocean sediments, the wavelength of the semidiurnal oscillation is about 35 cm, and that of the annual oscillation is about 9 m. At a depth of 1 wavelength, the amplitude of the oscillations is reduced by a factor of $\exp(-2\pi) = 0.002$ and so is negligible for bottom temperature variations of 1°C or less.

Over half of the oceanic heat flow measurements were made by the Scripps' Bullard-type probe with two thermisters located 1.7 m apart. The upper temperature sensor is usually located at about 15 cm beneath the recording case. Depending on the penetration conditions, the upper sensor can be anywhere above the sediment or buried up to a depth of about 30 cm in the sediment. The first temperature reading is thus subjected to the semidiurnal temperature disturbances and consequently may give erroneous heat flow values. The maximum relative error ϵ in heat flow due to a temperature fluctuation T_0 can be (from equation 8)

$$\epsilon = \pm T_0 \exp(-kz)/\Delta T \times 100\% \qquad (10)$$

where ΔT is the measured temperature difference. For example, a typical ΔT being about 0.1°C, $T_0 = 0.006$°C at depth 2500 m (Table 1, series 4) will give $\epsilon = \pm 6\%$, if $z = 0$; and ϵ is negligible at $z = 10$ cm. Nevertheless, it should be emphasized that T_0 can be many times larger than the values given in Table 1. The critical factor is the depth of burial z as it enters exponentially in (10). Therefore, deeper penetration and several temperature sensors are obviously desirable in oceanic heat flow measurements.

As for the annual temperature fluctuation, it diminishes rapidly with depth as indicated in Table 2. Consequently, it will not affect the oceanic heat flow measurements unless they are made in very shallow water (less than 1 km deep). Our results also demonstrate that heat flow measurements can be extended to shallow waters if care is taken to eliminate temperature fluctuations by deeper burial of the temperature gradient probe to about 3 m as advocated by *Lee et al.* [1966].

Finally, we wish to emphasize that longer continuous recordings of ocean water temperatures should be made to clarify the effects of thermal disturbances in the sediments and also the nature and causes of the temperature fluctuations. Such temperature recordings should also be made at various locations, especially over the mid-ocean ridges. The present analysis gives only a glance at the spectra of ocean water temperatures in the range of period between 5 hours and 4 days, and between 3 months and 3 years, leaving large segments not yet studied. Indeed, the frequency domain between those we investigated appears to be important because it contains the energetic current systems studied by *Swallow* [1961].

Appendix. Convection in the Boundary Layer of the Ocean Bottom

The continuity of heat flow at the water-sediment interface implies that a superadiabatic temperature gradient may exist in the boundary layer of the ocean bottom. This follows because the thermal conductivity of ocean sediments is approximately equal to that of ocean waters, and the geothermal gradient in the sediment is thousands of times greater than the adiabatic temperature gradient of ocean waters. However, the instability in shear associated with tidal motions (both of internal and ordinary tides) near the sea floor would be expected to create turbulences which would reduce the

superadiabatic temperature gradient in the water to a lower value.

The flux of heat through a boundary layer within a uniform fluid (e.g., seawater of uniform salinity) has been studied in great detail by meteorologists. According to the Monin-Obukhov 'similarity theory' [*Lumley* and *Panofsky*, 1964], the profiles of mean vertical velocity $U(z)$ and mean potential temperature $\theta(z)$ at a short distance z above the boundary are

$$U(z) = (\tau^{1/2}/k\rho^{1/2})[\ln(z/z_0) - \beta z/L] \quad (1)$$

$$\theta(z) - \theta_0 = -HU(z)/\tau C_p \quad (2)$$

where k is the von Kármán constant, τ the shear stress within the boundary layer, ρ the fluid density, β a constant determined empirically to be about 12, z_0 the roughness length of the bottom, L the modified Obukhov length, θ_0 the potential temperature at $z \approx z_0$, H the heat flux from the bottom, and C_p the specific heat at constant pressure.

The modified Obukhov length L is defined here as

$$L = \tau^{3/2}C_p/\rho^{1/2}g\alpha H \quad (3)$$

where g is the acceleration of gravity and α is the coefficient of thermal expansion. L is a parameter indicating forced or free convection because it is closely related to the height above the sea bottom at which the mechanical energy flux made available by the thermal expansion of the fluid is equal to the mechanical energy flux associated with the shear flow.

We can now use the average condition at the sea floor to determine whether the boundary layer of the ocean bottom is under forced or free convection, by computing L using (3). The least well-determined quantities are the shear stress τ and the roughness length z_0. Nevertheless, τ and z_0 are interrelated by

$$\tau = \rho\gamma^2 V^2 \quad (4)$$

where the resistance coefficient γ is

$$\gamma = k/\ln(z/z_0) \quad (5)$$

For a tidal current of velocity $V = 1$ cm/sec, $\tau = 10^{-3}$ dyne/cm^2, if we adopt $z_0 = 10^{-1}$ cm. Although the roughness length z_0 is very uncertain, it enters in the logarithmic factor in (5) and (1), so that τ and $U(z)$ are not too sensitive to its change of value. Other quantities appropriate for the sea floor at 5 km depth are $k = 0.4$, $H = 1.5 \times 10^{-6}$ cal/cm^2 sec, $\alpha = 1.7 \times 10^{-6}$ (°C^{-1}), and $C_p = 1$ cal/g °C. These values lead to

$$L \approx 10^4 \text{ cm} \quad (5)$$

Such a large modified Obukhov length L implies that the convection of heat in the boundary layer of the ocean bottom is *forced* by the turbulence motion associated with tides because its thickness is much less than 100 m.

We can also estimate the differences between the temperatures at ocean floor and at various heights z above it and the maximum vertical potential temperature gradient ($\partial\theta/\partial z$) that can exist. Using (2) we obtain for various z the following:

z, cm	10	10^2	10^3
$U(z)$, cm/sec	0.36	0.54	0 63
$\theta(z) - \theta_0$, °C	-5.4×10^{-4}	-8.1×10^{-4}	-9.4×10^{-4}
$\partial\theta/\partial z$, °C/cm	-5.4×10^{-5}	-8.1×10^{-6}	$-9\ 4 \times 10^{-7}$

Since the adiabatic gradient for deep ocean water is about 1.3×10^{-6} °C/cm, the above results imply that large superadiabatic gradients cannot exist for much over 1 m above the sea floor. We wish to emphasize, however, that one cannot rule out the possibility of large *local* superadiabatic gradients near the ocean bottom. Their existence, if confirmed, may indicate that the seawater is prevented from turbulence motion by factors such as a stabilizing density gradient.

Acknowledgments. We wish to thank R. S. Arthur, E. C. Bullard, T. D. Foster, A. H. Lachenbruch, L. J. Lynn, J. L. Reid, R. O. Reid, and R. P. Von Herzen for their helpful comments on the manuscript.

This work was supported by a grant from the National Aeronautics and Space Administration (NsG 216-62) and by the Office of Naval Research.

References

Blackman, R. B., and J. W. Tukey, *The Measurement of Power Spectra,* Dover Publications, New York, 1958.

Bullard, E. C., and A. Day, The flow of heat through the floor of the Atlantic Ocean, *Geophysics. J., 4,* 282–292, 1961.

Carslaw, H. S., and J. C. Jaeger, *Conduction of Heat in Solids,* 2nd ed., Oxford University Press, London, 1959.

Cox, C. S., and H. Sandstrom, Coupling of internal and surface waves in water of variable depth, *Oceanog. Soc. Japan, J., 20th Anniversary Vol.*, 499–513, 1962.

Cox, C. S., B. P. Johnson, H. Sandstrom, and J. H. Jones, A taut wire mooring for deep temperature recordings, in *Ocean Science and Ocean Engineering, Trans. Joint Conf. in June 1965 by Marine Technol. Soc. and Am. Soc. Limnol. and Oceanog.*, vol. 2, pp. 990–998, 1965.

Crease, J., Velocity measurements in the deep water of the western North Atlantic, *J. Geophys. Res., 67*, 3173–3176, 1962.

Defant, A., Die Gezeiten und inneren Gezeitenwellen des Atlantischen Ozeans, *Wiss. Ergebn. Deut. Att. Exp. "Meteor," 1925–27, 7*(1), 1–318, 1932.

Defant, A., On the origin of internal tide waves in the open sea, *J. Marine Res., 9*(2), 111–119, 1950.

Haurwitz, B., H. Stommel, and W. H. Munk, On the thermal unrest in the ocean, in *The Atmosphere and the Sea in Motion*, edited by B. Bolin, pp. 74–94, Rockefeller Institute Press, New York, 1959.

Jenkins, G. M., General considerations in the analysis of spectra, *Technometrics, 3*, 133–166, 1961.

Lee, W. H. K., and S. Uyeda, Review of heat flow data, in *Terrestrial Heat Flow*, edited by W. H. K. Lee, *Geophys. Monograph 8*, 87–190, American Geophysical Union, Washington, D. C., 1965.

Lee, W. H. K., S. Uyeda, and P. Taylor, Geothermal studies of continental margins and island arcs, *Bull. Can. Geol. Surv.*, in press, 1966.

Longuet-Higgins, M. S., Planetary waves on a rotating sphere, *Proc. Roy. Soc. London, A., 284*, 40–54, 1965.

Lubimova, E. A., R. P. Von Herzen, and G. B. Udintsev, On heat transfer through the ocean floor, in *Terrestrial Heat Flow*, edited by W. H. K. Lee, *Geophys. Monograph 8*, 78–86, American Geophysical Union, Washington, D. C., 1965.

Lumley, J. L., and H. A. Panofsky, *The Structure of Atmospheric Turbulence*, pp. 99–118, Interscience Publishers, New York, 1964.

Munk, W. H., F. E. Snodgrass, and M. J. Tucker, Spectra of low-frequency ocean waves, *Bull. Scripps Inst. Oceanog., 7*, 283–362, 1959.

Rattray, M., Time dependent motion in an ocean, *Studies in Oceanography*, pp. 19–29, Geophysical Institute, Tokyo University, 1964.

Reid, J. L., Observations of internal tides in October 1950, *Trans. Am. Geophys. Union, 37*, 278–286, 1956.

Reid, J. L., and R. J. Lynn, The distribution of water properties at deep and abyssal depths beneath the California current, *Final Report to the U. S. Atomic Energy Commission, UCSD-34P97-1*, 1965.

Rossby, C. G., On the mutual adjustment of pressure and velocity distribution in certain simple current systems, *J. Marine Res., 1*, parts 1 and 2, 15–28, 239–263, 1937–1938.

Swallow, J. C., Ocean circulation, *Sci. Progr. (London), 49*, 281–285, 1961.

Von Herzen, R. P., and M. G. Langseth, Present status of oceanic heat flow measurements, *Phys. Chem. Earth, 6*, 365–408, 1965.

Von Herzen, R. P., and A. E. Maxwell, Measurements of heat flow at the preliminary Mohole site off Mexico, *J. Geophys. Res., 69*, 741–748, 1964.

(Manuscript received November 9, 1965;
revised December 27, 1965.)